Journal of Molecular Graphics and Modelling 38 (2012) 342–353

Contents lists available at SciVerse ScienceDirect

Journal of Molecular Graphics and Modelling

journal homepage: www.elsevier.com/locate/JMGM

Identification of structural determinants of ligand selectivity in 5-HT_2 receptor subtypes on the basis of protein–ligand interactions

Jae Wan Jang[a,b], Min Sup Kim[c], Yong Seo Cho[a], Art E. Cho[c], Ae Nim Pae[a,b,*]

[a] Center for Neuro-Medicine, Brain Science Institute, Korea Institute of Science and Technology, PO Box 131, Cheongryang, Seoul 130-650, Republic of Korea
[b] Department of Medicinal and Pharmaceutical Chemistry, School of Science, University of Science and Technology, 52 Eoeun dong, Yuseong-gu, Daejeon 305-333, Republic of Korea
[c] Department of Biotechnology and Bioinformatics, Korea University, Jochiwon, Chungnam 339-700, Republic of Korea

ARTICLE INFO

Article history:
Accepted 13 June 2012
Available online 10 July 2012

Keywords:
5-HT_2 receptor
Subtype selectivity
Homology modeling
Protein–ligand docking
Molecular dynamic simulation

ABSTRACT

Drug selectivity is one of the most critical improvement steps in drug development. The 5-hydroxytryptamine 2 (5-HT_2) receptor has 3 subtypes that exhibit different pharmacological functions. Because of their high amino acid sequence similarity, designing small molecules that selectively activate only 1 receptor among the 3 subtypes is difficult. We performed homology modeling of the 5-HT_2 receptor subtypes using the β_2-adrenergic receptor as a template to identify differences in active sites that may influence 5-HT_2 receptor agonist selectivity. A subset of selective 5-HT_2 agonists was docked into the modeled protein structures to investigate their interactions with each receptor. Subtype-specific active site residues at positions xl2.54, 5.39, and 5.46 interacted differently with each ligand. Molecular dynamics simulations revealed that position 5.46 of the 5-HT_{2A} receptor interacted more favorably with selective 5-HT_{2A} agonists than with selective 5-HT_{2B} agonists. These computationally obtained insights provided clues to improving agonist selectivity for specific pharmacological action at 5-HT_2 receptors.

1. Introduction

The G-protein coupled receptors (GPCRs) have attracted attention as a drug target because of their roles in signaling pathways. More than 30% of the top 20 drugs in U.S. sales target are GPCRs [1], which are characterized by 7 transmembrane-spanning regions and recognized by various types of effectors such as ions, small molecules, peptides, and globular proteins [2]. GPCRs can be divided into 5 classes, each of which is divided into subfamilies and types [3]. Owing to high binding site similarities between GPCRs of the same subtype, a single endogenous ligand often stimulates several GPCR targets at the same time [4]. This orthosteric binding site similarity poses a problem for researchers seeking to develop subtype-selective GPCR ligands. Novel GPCR drugs must be highly selective to the subtypes to reduce unwanted side effects.

The serotonin receptors are members of the GPCR family, and include 7 member subtypes, i.e., 5-HT_1 to 5-HT_7. They are involved in a variety of biological functions, such as intestinal movement [5] and cognitive functions such as mood, appetite, and sleep [6,7]. 5-HT_2 has 3 subtypes: 5-HT_{2A}, 5-HT_{2B}, and 5-HT_{2C}. 5-HT_{2A} is widely expressed in the brain, especially in the cerebral cortex, and is implicated in the hallucinogenic action of drugs such as lysergic acid diethylamide (LSD) [8,9]. Drugs targeting 5-HT_{2A} have been developed for the treatment of schizophrenia and insomnia [9]. The 5-HT_{2B} receptor is found in the cardiovascular system and is associated with the lethal valvulopathy that is a side effect of some prescription drugs [10–13]. The 5-HT_{2C} receptor is found in high concentrations exclusively in the central nervous system, and drugs targeting this receptor have been developed for the treatment of depression, anxiety, eating disorders, obsessive–compulsive disorder, chronic pain conditions, obesity, epilepsy, and erectile dysfunction [14–23]. Since these 3 subtypes have high sequence similarity and similar pharmacological functions [5,24], it is difficult to design a drug that selectively binds to only 1.

To uncover the structural basis of drug selectivity in the three 5-HT_2 subtypes, we employed homology modeling, protein–ligand docking, and molecular dynamics simulation. Rashid et al. attempted to reveal the structural basis of 5-HT_2 subtype selectivity by using homology modeling and molecular dynamics simulation; however, they employed the crystal structure of bovine rhodopsin as a template, as it was the only crystal structure available [24–26]. Now, 9 GPCR X-ray crystal structures have been released: β_1-adrenergic receptor, β_2-adrenergic receptor, adenosine A_{2A} receptor structures, dopamine D_3 receptor, CXCR4 chemokine receptor, histamine H1, M2 muscarinic acetylcholine, μ-opioid, and κ-opioid receptor [27–38]. More recently reported structures differ from the crystal structure of bovine rhodopsin particularly in extracellular loop 2 (EL2), which exhibits variable

* Corresponding author at: Center for Neuro-Medicine, Brain Science Institute, Korea Institute of Science and Technology, PO Box 131, Cheongryang, Seoul 130-650, Republic of Korea. Tel.: +82 2 958 5185; fax: +82 2 958 5189.
E-mail address: anpae@kist.re.kr (A.N. Pae).

1093-3263/$ – see front matter © 2012 Elsevier Inc. All rights reserved.
http://dx.doi.org/10.1016/j.jmgm.2012.06.006

topology between species. The role of EL2 in ligand binding was reported by Reynolds et al. They demonstrated that a GPCR protein model based on the β_2-adrenergic receptor outperforms the model based on bovine rhodopsin in virtual screening simulations because of the role of EL2 in ligand interaction [39]. To obtain the most reliable helix arrangement and topology and loop conformation of serotonin receptors, we tested all available templates with our targets, and selected the most plausible one for homology modeling. All three 5-HT_2 receptor subtypes were generated and superimposed to identify the amino acid differences that might cause 5-HT_2 agonist selectivity. On these structures, protein–ligand docking simulations were carried out with diverse selective 5-HT_2 agonists to elucidate how the different residues influence ligand selectivity. Further, molecular dynamics simulation studies made us confident in our identification of the 5-HT_{2A} residue for 5-HT_{2A} agonist selectivity. Comparing the amino acid sequences and 3-dimensional structures, and investigating each protein–ligand interaction by docking and molecular dynamics simulation suggested the molecular basis for 5-HT_2 agonist selectivity.

2. Methods

2.1. Comparative 3-dimensional modeling

2.1.1. Template selection and sequence alignment

The sequences of the human 5-HT_{2A} (P28223), 5-HT_{2B} (P41595), and 5-HT_{2C} (P28335) receptors were retrieved from the Uni-Prot database (http://www.uniprot.org/). All GPCR crystal structures including that of bovine rhodopsin were collected as a template from the Protein Data Bank (PDB, http://www.pdb.org/): 3PBL, 1F88, 3ODU, 2RH1, 2VT4, and 3EML. Each template was aligned to the target sequence with the automated alignment tool, ClustalW [40]. The DRY motif in transmembrane region 3 and residue W6.48 were fixed to minimize misalignment. After alignment of all templates was complete, sequence identity and similarity between each template and target were compared to find the best template. Special attention was given to 10 residues in the putative binding sites: W130, D134, S138, V215, S219, A222, W324, F328, N331, and Y358. The selected alignment with the best template was treated carefully with some adjustment. Using Swiss-Prot (http://www.expasy.ch) and TMPRED (http://www.ch.embnet.org), we predicted the TM regions of the target sequences, and the TM region alignments were checked for correct alignment. Mismatches in the highly conserved residues of the GPCR superfamily, as explained by Baldwin et al. [41], were corrected manually.

2.1.2. Single and static 3-dimensional model generation for each subtype

Three-dimensional models of 5-HT_{2A}, 5-HT_{2B}, and 5-HT_{2C} were generated by homology modeling. The best alignment result and template input into MODELLER 9v4 [42] in Discovery Studio 2.5 (http://accelyrs.com). Since the disulfide bridge between Cys3.25 (numbering scheme by Ballesteros and Weinstein [43]) and Cysxl2.50 (the second extracellular loop 2) is highly conserved among GPCR receptors, they were constrained during model generation. The "Refine Loops" option of MODELLER was used for loop refinement, and 10 different loop conformations were produced for each structure. In total, 100 candidate models for each receptor were initially generated and sorted by the total probability density function (PDF) of MODELLER. Out of these 100 models, the models with the 10 lowest-energy PDF were selected, and their side chains were refined using local rotamer libraries [44]. Minimization of these structures was performed with the OPLS_2001 force field [45] in the Schrödinger package. During minimization, the protein backbones were fixed to prevent collapse of the small GPCR binding sites. To select the best structure from these candidates, we employed site-directed mutagenesis data for each of the 5-HT_2 subtypes. Structures that did not satisfy these data were discarded. To select the final model, the most plausible loop conformation was selected from 10 different conformations. The second extracellular loop region was the only loop region considered because of its potential interaction with ligands. After loop optimization, PROCHECK [46] and QPACK [47] analyses were used to validate the geometry of the residues.

2.2. Ligand preparation and molecular docking

All ligand structures were generated with Maestro 9.0 [48], which is part of the Schrödinger package. After drawing the ligand structures, the Ligprep module of Maestro was utilized for 3-dimensional coordinate optimization. They were assigned protonation states at pH 7.4. ConfGen [49] was employed to account for all low-energy ligand conformations. All ligand structures were minimized using the OPLS_2001 force field. Ligands were docked into the protein structure using Glide XP [50]. A receptor grid was generated before docking the compounds. An outer box was used to generate the grid and accommodating ligands, and an inner box was used for ligand center site point search. The outer and inner boxes were set to lengths of less than 20 Å and 10 Å, respectively. For grid generation, the scaling factor for receptor atom van der Waals radius was set to 1.0. Since most of the 5-HT ligands have a hydrogen bond functional group as a counterpart to residue D3.32, we selected this residue as the centroid of the outer box, which confined the ligand during Glide docking. The D3.32 carbonyl oxygen atom was constrained to accept a hydrogen bond from the ligand. This hydrogen bond constraint was used in all docking calculations.

2.3. Molecular dynamics simulations

We performed molecular dynamics (MD) simulation to observe interaction changes in the binding mode produced by docking simulation. We used Desmond 3.0 in the Schrödinger package and Maestro's trajectory visualizer. Each MD simulation was initiated by building the MD model. The MD model had a cell size of $56.4 \times 73.8 \times 79.2$ Å, and was constrained to be orthorhombic. The predicted structure of the agonist-bound form was independently embedded in a square periodic lipid bilayer consisting of palmitoyloleoyl phosphatidylcholine (POPC) molecules. The system was solvated with the TIP3P water model; in total, the MD system contains approximately 65,000 atoms. We used OPLS-2005 force field parameters for all calculations, and balanced the charge of the system by replacing some of the water molecules with chloride ion using the Ion neutralize option.

All MD systems were minimized before the simulation. This minimization step was performed by using the "relax model system before simulation" option as a default protocol in Desmond. This step consists of repetitive minimization and molecular dynamics simulation stages, so that all of the model system is relaxed before simulation. First, minimization was carried out with solute restrained. Then, the system was minimized again without restraints. Next, 12 ps MD simulation was performed with the NVT ensemble using a Berendsen thermostat at 10 K. The 12 ps MD simulation was repeated with the NPT ensemble using a Berendsen thermostat and a Berendsen barostat at 10 K and 1 atm. Finally, 24 ps MD simulation was performed with the NPT ensemble using a Berendsen thermostat and a Berendsen barostat at 300 K and 1 atm.

We carried out the main MD simulation using NVT ensemble with the Nose-Hoover thermostat method set at 300 K reference temperature. The energy was calculated at every 1.2 ps of MD simulation, and the trajectory was calculated every 4.8 ps. Total

Table 1
Sequence identity between targets and templates.

Target	Condition	Template					
		1F88	2RH1	2VT4	3EML	3PBL	3ODU
5-HT_{2A}	Active	20%	80%	80%	30%	70%	10%
	Overall	16.8%	21.7%	24.6%	18.7%	24.8%	13.9%
5-HT_{2B}	Active	10%	70%	70%	20%	50%	10%
	Overall	15.2%	22.9%	23.9%	19.0%	22.5%	14.5%
5-HT_{2C}	Active	20%	70%	70%	30%	60%	10%
	Overall	16%	25.3%	25.1%	16.9%	25.8%	16.7%

The PDB code was used to represent each template: 1F88, bovine rhodopsin; 2RH1, human β_2-adrenergic receptor; 2VT4, human β_1-adrenergic receptor; 3EML, adenosine A_{2A} receptor; 3PBL, dopamine D3 receptor; 3ODU, CXCR4 chemokine receptor. The active site was based on 10 positions previously identified by site-directed mutagenesis. Those positions are 3.28, 3.32, 3.36, 5.39, 5.43, 5.46, 6.48, 6.52, 6.55, and 7.43 according to the Ballesteros–Weinstein numbering scheme. Accurate alignment of each template and target sequences was achieved by fixing the DRY motif of TM3 between target and template.

MD simulation time for salt bridge distance measurement and protein–ligand interaction distance was 10 ns. Every 100 ps, a snapshot was written to the trajectory file for analysis.

3. Results and discussion

3.1. Sequence comparison by alignment

All available template structures were employed and compared with the target to avoid the biased results of comparative protein modeling. Since the purpose of our study was to investigate agonist binding site interaction for subtype selectivity, we calculated not only the sequence identity as a whole, but also that of the active site. As shown in Table 1, 2RH1, 3PBL, and 2VT4 were suitable templates, having an overall identity of ≥20%. Active site consideration alone suggests that both 2RH1 and 2VT4 have ~10–20% greater sequence identity with the template than 3PBL, indicating ~1–2 residues share greater identity. Fig. 1 illustrates our observation that β-adrenergic receptors share the greatest identity with 5-HT_2 receptors for the ligand-binding amino acids identified by site-directed mutagenesis. We chose to use β_2-adrenergic receptor 2RH1 as the best template, because it has a higher crystallographic resolution than the β_1-adrenergic receptor 2VT4; in addition, 2RH1 originated from humans while 2VT4, from turkey.

The initial alignment was performed automatically and adjusted manually based on the conserved GPCR domain. The final alignment revealed total sequence identity and similarity between the targets

Sequence Alignment

		TM3	TM5	TM6	TM7
		3.28 3.32 3.36	5.39 5.43 5.46	6.48 6.52 6.55	7.43
Target	**5HT2A**	WDS	VSS	WFN	Y
	5HT2B	WDS	MSA	WFN	Y
	5HT2C	WDS	VSA	WFN	Y
Template	**1F88**	EAG	VFH	WAA	K
	2RH1	WDV	ASS	WFN	Y
	2VT4	WDV	ASS	WFN	Y
	3EML	IVT	VFC	WHN	H
	3PBL	FDC	VSS	WFH	Y
	3ODU	VYL	QIG	WYI	I

Fig. 1. Amino acid alignment in the active sites of 6 crystal structures and 5-HT_{2A}, 5-HT_{2B}, and 5-HT_{2C}. 1F88, Bovine rhodopsin; 2RH1, human β_2-adrenergic receptor; 2VT4, human β_1-adrenergic receptor; 3EML, adenosine A_{2A} receptor; 3PBL, dopamine D3 receptor; 3ODU, CXCR4 chemokine receptor. The Ballesteros-Weinstein numbering scheme was used to represent the GPCR amino acids.

and template were 22.8%/39.9% (5-HT_{2A}), 22.3%/39.7% (5-HT_{2B}), and 24.9%/43.1% (5-HT_{2C}). The sequence similarities increased by almost 2-fold when only the transmembrane regions were considered (5-HT_{2A}: 39.1%/62.8%, 5-HT_{2B}: 37.7%/62.3%, 5-HT_{2C}: 41.4%/64.7%). Remarkably, the sequences in the putative ligand binding site regions are highly similar (~60–80% identity), indicating the high reliability of the template for homology modeling (Table 1). The sequence alignment also revealed the possible origins for selectivity-regions in which residues differed between subtypes. We identified residues that interact with ligands on the basis of the ligand-docking simulation. These residues are colored pink in Fig. 2. All are the same residue type except at 3 locations. The first variation is in the EL2 region: xl2.54. It is well known that the loop regions carry large mutations even within a subtype. The residues are the aspartate in 5-HT_{2A}, lysine in 5-HT_{2B}, and asparagine in 5-HT_{2C}. The other variable residues are found in the transmembrane domain positions: 5.39 and 5.46. At 5.39, valine in 5-HT_{2A} and 5-HT_{2C} is replaced by methionine in 5-HT_{2B}. Position 5.46 is occupied by serine in 5-HT_{2A} and by alanine in 5-HT_{2B} and 5-HT_{2C}. They differ in charge state, polarity, and hydrophobicity, suggesting a possible role in selectivity. For example, the aspartate at xl2.54 of 5-HT_{2A} possesses a negatively charged carboxylate group capable of hydrogen bonding, whereas the lysine at the same position of 5-HT_{2B} is positively charged and more spatially constrained owing to its large flexibility, and the asparagine in 5-HT_{2C} is polar but uncharged and can act either as a hydrogen bond donor or acceptor. In the 5.46 region, only the serine in 5-HT_{2A} is polar, also suggesting a possible role in ligand selectivity. In the 5.39 regions, although they have similar properties (both methionine and valine have non-polar and aliphatic R-groups), their length and flexibility are dissimilar, implying different ligand interactions. Consequently, xl2.54, 5.39, and 5.46 were considered important for the docking simulation.

Identical residues are darkly shaded, and closely related residues are lightly shaded. The most conserved residues among the GPCR super-family and cysteine residues of the disulfide bridge between the second extracellular loop region and the third transmembrane region are shown in bold with a caret symbol. Residues involved in ligand binding are colored pink and are numbered according to the Ballesteros-Weinstein scheme.

3.2. Selection of candidate models for each subtype: site-directed mutagenesis data

Using the sequence alignment above, we constructed 3-dimensional protein models for each 5-HT_2 subtype. To select the native-like protein model conformations from the pool generated with the MODELLER algorithm, 2 criteria were employed. First, we selected the most energetically favorable conformation based on the assumption that the lowest energy conformation is near the native structure [51]. We thus obtained the 10 lowest-energy conformations of each 5-HT_2 subtype measured by the PDF in MODELLER. Then, the site-directed mutagenesis data for each receptor subtype were employed to select the most reliable model. These data have been reported in several pharmacology papers. We collected the data, summarized in Table 2. We considered a model reliable if the ligand docking results agreed with the site-directed mutagenesis data [52–54]. Docking simulations showed that some of the homology models missed interactions described in the mutagenesis data. As for 5-HT_{2A}, 3 models ideally reproduced the ligand interactions identified in the mutagenesis data, while in the case of 5-HT_{2B}, 4 models perfectly generated the 5-hydroxytryptamine interaction, and only 2 homology structures of 5-HT_{2C} exhibited ligand-binding modes consistent with the mutagenesis data (see supplementary information). Ramachandran plots of the models, 5-HT_{2A}, 5-HT_{2B}, and 5-HT_{2C} showed 88.7%, 91.7%, and 92.8% residues

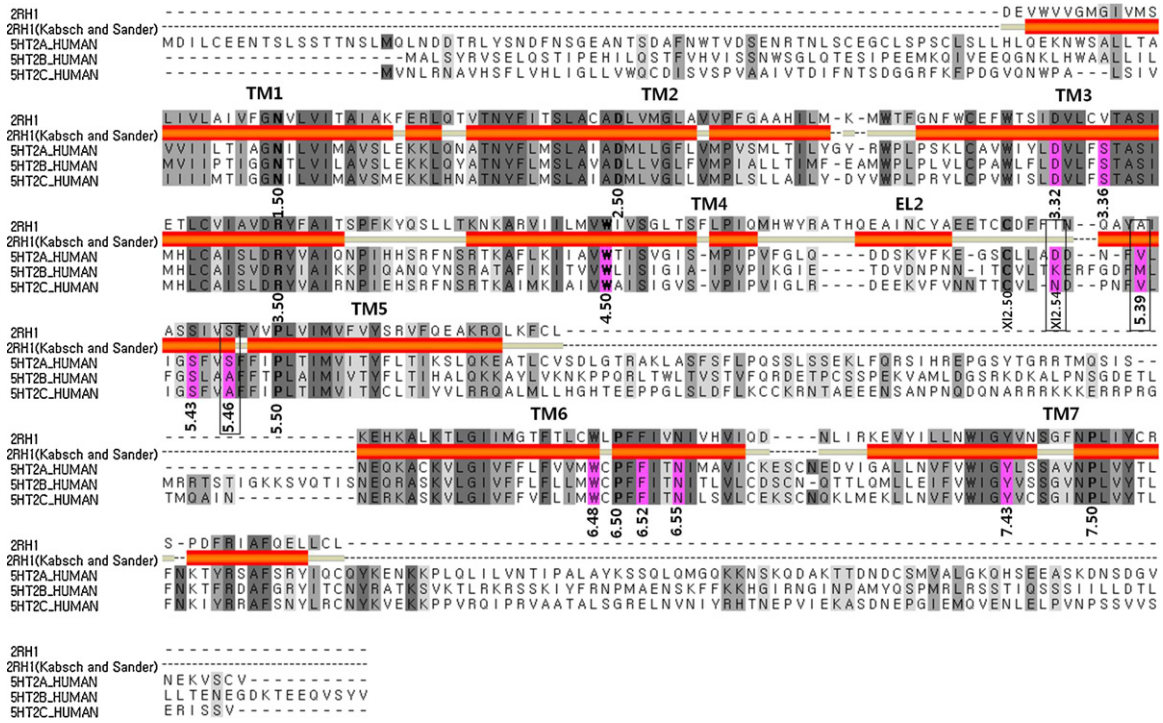

Fig. 2. Multiple sequence alignment of the human 5-HT_{2A}, 5-HT_{2B}, 5-HT_{2C}, and β_2-adrenergic receptors.

Table 2
Summary of the site-directed mutagenesis data in human 5-HT_2 subtypes. Residues that affected ligand affinity are listed in the table. Residues were numbered according to the Ballesteros–Weinstein scheme.

	Ligands used for mutagenesis studies				
	5-Hydroxytryptamine	Ergolines	Mesulergine	*D*-LSD[a]	Ketanserin
5-HT_{2A}	D3.32, S3.36, S5.43, S5.46, W6.48, Y7.43, W7.40	–	–	S5.46	W6.48, D3.32, F6.52
5-HT_{2B}	D3.32, S3.36, F6.52, N6.55, D7.36	–	–	–	–
5-HT_{2C}	D3.32, S3.36, F6.52	A5.46	A5.46	–	–

[a] *D*-LSD: dextro-lysergic acid diethylamide.

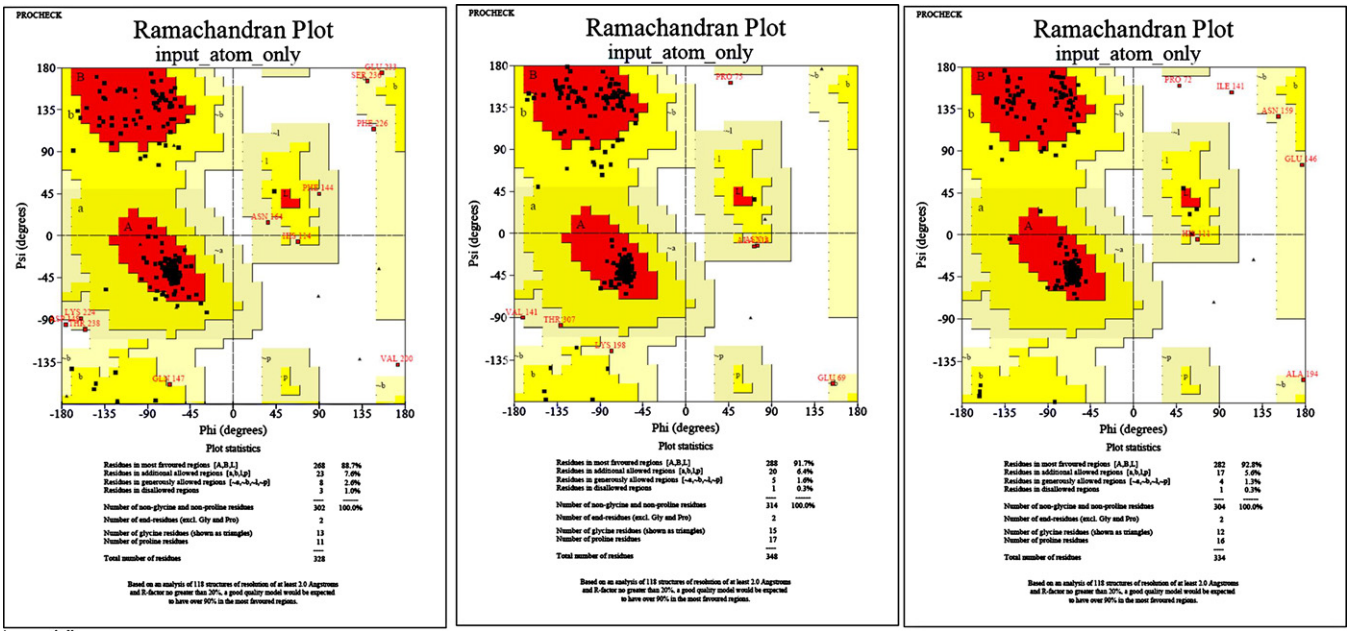

Fig. 3. Ramachandran plots of the homology models for (A) 5-HT_{2A}, (B) 5-HT_{2B}, and (C) 5-HT_{2C} (c). The most favored regions are red and the disallowed regions are white.

in the most favored region (Fig. 3), which was acceptable. Fig. 4 illustrates the comparison of superimposed structures of three 5-HT_2 subtype models. We can see 3 regions identified from the sequence alignment with differences in their residue identities. All are located in the inner region of the ligand binding pocket and are likely to participate in ligand interactions.

Residues involved in ligand binding and receptor activation are displayed. The Ballesteros–Weinstein scheme was applied to the residue labeling; if residue identity differed between subtypes, that of 5-HT_{2A} was listed first, followed by those of 5-HT_{2B} and 5-HT_{2C}. The figure was generated using PyMol (http://www.pymol.org). Green: 5-HT_{2A}, Sky blue: 5-HT_{2B}, Pink: 5-HT_{2C}.

3.3. Docking of 5-HT_2 agonists to each receptor

To investigate the role of the identified residues in 5-HT_2 agonist selectivity, docking simulations of known selective compounds to each of the receptor subtypes were performed. In 2004, Knight et al. reported comprehensive agonist radioligand binding assays under the same conditions and with receptors from the same species (Fig. 5) [55]. We employed these compounds and the corresponding binding affinity data in our docking studies. Since some 5-HT_2 agonists have similar binding affinity to several subtypes at the same time, we selected only highly selective agonists that are well known. The docking scores of all compounds with experimental

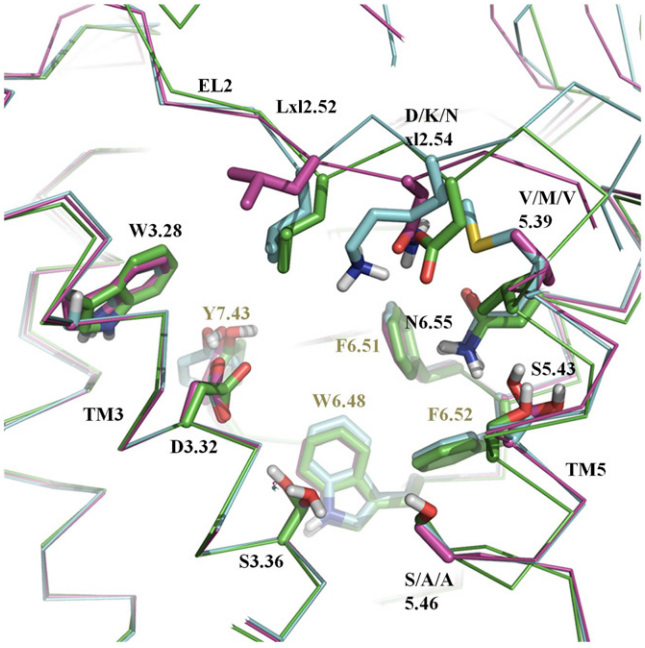

Fig. 4. Superimposition of the 5-HT_{2A}, 5-HT_{2B}, and 5-HT_{2C} structures generated by homology modeling.

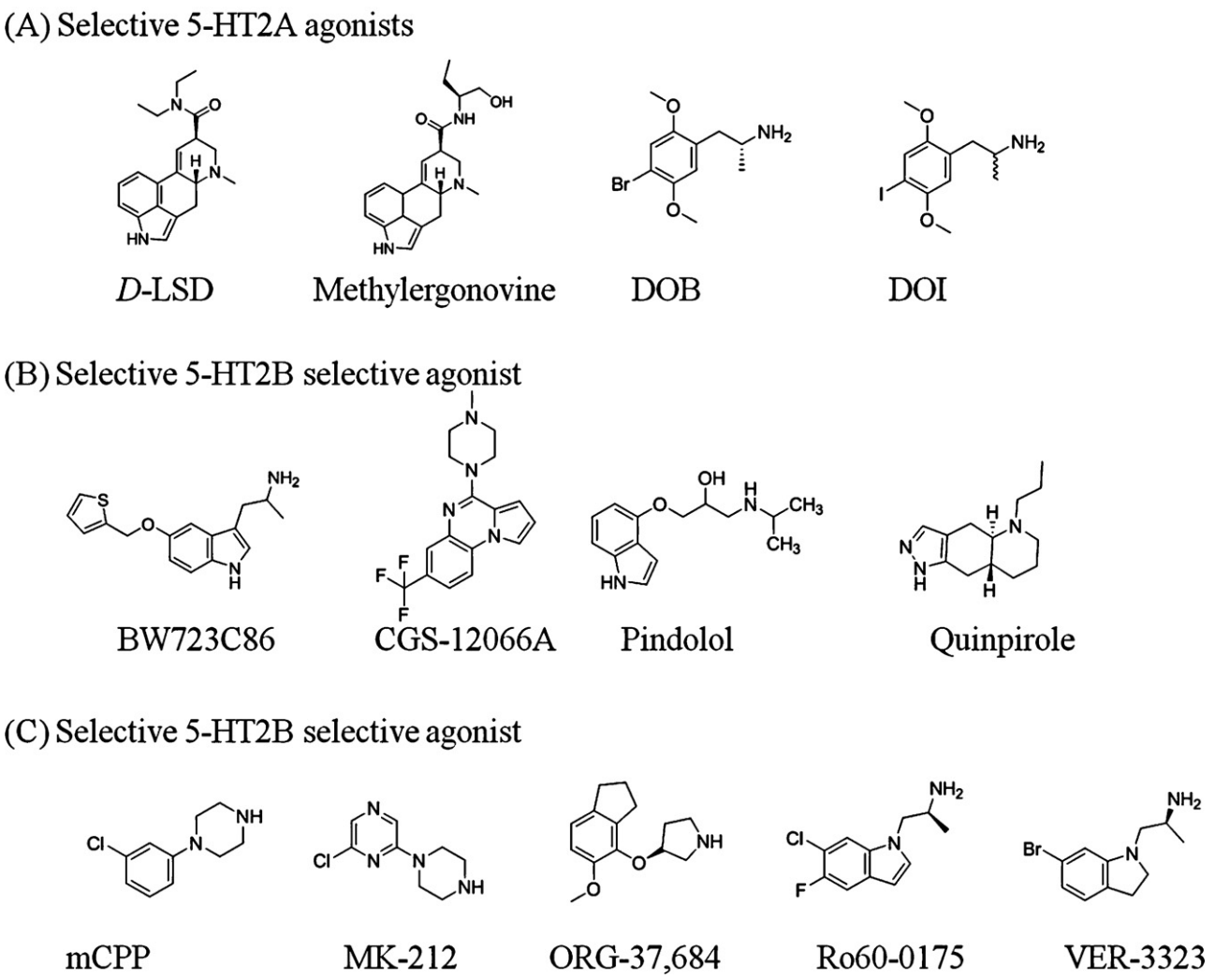

Fig. 5. 5-HT_2 receptor agonists for docking studies.

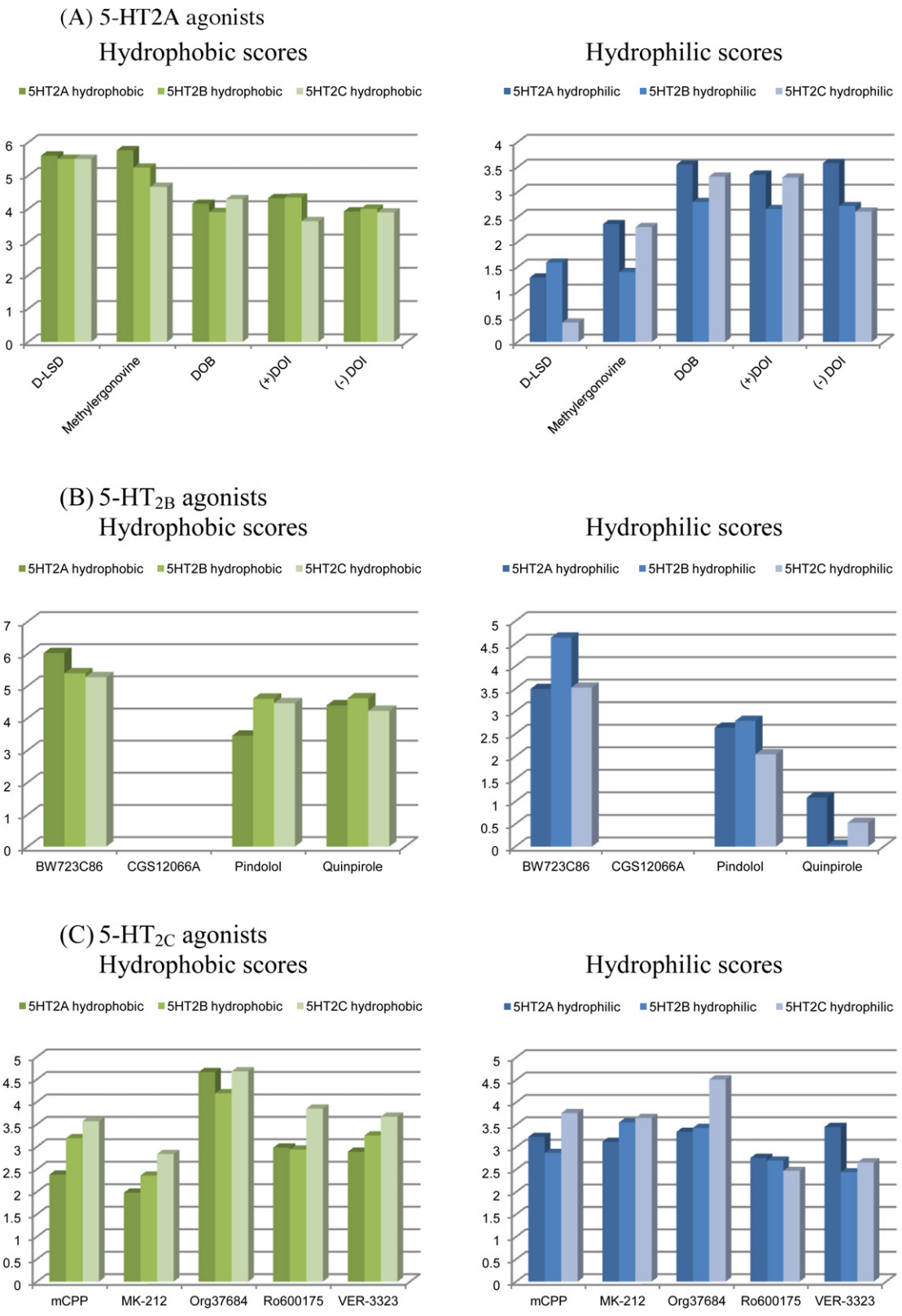

Fig. 6. Graphical plot of hydrophobic and hydrophilic components of the Glide XP score of 5-HT_2 agonists used for docking studies. Hydrophobic score indicates the sum of "LipophilicEvdW" and "PhoEn" Gscore component terms and hydrophilic score is the sum of "HBond" and "Electro". Green bar denotes the hydrophobic score and blue bar indicates the hydrophilic score. *Y*-axis indicates the converted positive value of the glide score. The higher score is therefore more energetically favorable. With the exception of D-LSD, all hydrophilic scores of 5-HT_{2A} agonists have the highest scores at the 5-HT_{2A} receptors, and all 5-HT_{2C} agonists produce the highest hydrophobic scores at 5-HT_{2C} receptors.

Table 3
Summary of docking scores and experimental biological affinities of docked compounds. Docking score and experimental biological affinity of selective 5-HT_2 agonists. All biological affinities are *Ki* values for agonist ligands at the agonist-preferring radioligand binding site of 3 subtypes of human recombinant 5-HT2 receptor [55].

Category	Ligand	Gscore			Experimental biological affinity		
		5-HT_{2A}	5-HT_{2B}	5-HT_{2C}	5-HT_{2A}	5-HT_{2B}	5-HT_{2C}
Selective 5-HT_{2A} agonist	*D*-LSD	−9.415	−8.35	−7.016	9.12 ± 0.06	9.01 ± 0.09	8.96 ± 0.06
	Methylergonovine	−10.44	−7.90	−8.99	9.45 ± 0.11	9.34 ± 0.07	8.34 ± 0.06
	DOB	−10.13	−9.12	−10.03	8.93 ± 0.07	7.36 ± 0.04	8.20 ± 0.06
	(+) DOI	−10.04	−9.37	−9.29	9.03 ± 0.11	7.55 ± 0.05	8.08 ± 0.11
	(−) DOI	−9.86	−9.09	−8.88	9.19 ± 0.12	7.27 ± 0.06	8.27 ± 0.12
Selective 5-HT_{2B} agonist	BW723C86	−11.026	−12.26	−11.04	7.20 ± 0.08	7.33 ± 0.03	7.11 ± 0.21
	CGS12066A	–	–	–	5.37 ± 0.06	6.06 ± 0.09	5.60 ± 0.09
	Pindolol	−8.12	−9.05	−8.52	5.03 ± 0.14	5.66 ± 0.22	<5.00
	Quinpirole	−6.98	−6.15	−6.26	5.48 ± 0.10	6.52 ± 0.06	5.48 ± 0.05
Selective 5-HT_{2C} agonist	mCPP	−5.48	−7.93	−9.20	7.26 ± 0.02	7.39 ± 0.02	7.85 ± 0.07
	MK-212	−6.97	−7.79	−8.37	5.99 ± 0.06	6.21 ± 0.09	7.01 ± 0.09
	Org37684	−7.82	−9.43	−11.01	7.49 ± 0.08	7.37 ± 0.06	8.12 ± 0.20
	Ro600175	−8.59	−8.41	−9.06	7.44 ± 0.04	8.27 ± 0.06	8.22 ± 0.29
	VER-3323	−6.84	−8.18	−8.83	6.45 ± 0.04	7.52 ± 0.04	8.25 ± 0.05

binding affinities are summarized in Table 3. The scores are concordant with the experimental affinities at 5-HT_{2A} and 5-HT_{2C}, as the ligands known to be selective for a certain subtype produced the highest scores at that subtype. In the case of 5-HT_{2B} agonists, one ligand failed to find the suitable conformation, and another ligand showed an unexpected docking score, as it seems to occur because of low experimental binding affinity of these compounds to the 5-HT_{2B} receptor. The piperazine of CGS-12066A, which was the compound that failed to dock, might have formed a hydrogen bond with D3.32, but its trifluoro methyl moiety seems to be too bulky to be accommodated by the binding pocket, resulting in docking failure. Quinpirole, which also had an unexpected score, displayed the highest score at the 5-HT_{2A} receptor, although it is a selective 5-HT_{2B} agonist. In addition, we extracted the hydrophobic and hydrophilic components of the docking score and compared them with each other to observe important interactions determining the selectivity of those docked compounds (Fig. 6). Several terms in the Glide XP docking score calculate the hydrophobic and hydrophilic interactions. "LipophilicEvdW" and "PhoEn" describe the hydrophobic component, and "HBond" and "Electro" calculate the hydrophilic component. "LipophilicEvdW" refers to lipophilicity as derived from the hydrophobic grid potential and a fraction of the total protein–ligand vdW energy, while "PhoEn" represents the hydrophobic enclosure reward term if the ligand structure is surrounded by hydrophobic residues. "HBond" is a ChemScore H-bond pair term, and "Electro" describes electrostatic interactions between ligand and receptor atoms. The hydrophilic score, which is a summation of the "HBond" and "Electro" scores, showed that, with the exception of D-LSD, 5-HT_{2A} agonists displayed the highest hydrophilic score at 5-HT_{2A} receptor, implying a certain role of hydrophilicity in determining 5-HT_{2A} agonist selectivity (Fig. 6(A)). In the case of 5-HT_{2C}, the hydrophobic scores of all 5-HT_{2C} agonists were highest at 5-HT_{2C} receptors, indicating the hydrophobicity of the binding pocket (Fig. 6(C)). The subtype-selective residues Ser5.46 of 5-HT_{2A} and Ala5.46 of 5-HT_{2C} in the binding mode explains the docking score trend described in the next section.

3.4. Docking of 5-HT_{2A} agonists

We selected 4 compounds for our 5-HT_{2A} agonist selectivity studies. It has been reported that LSD and indolealkylamines, including DOB and DOI, activate 5-HT_{2B} and are hallucinogenic in humans [56–59]. We also chose methylergonovine because it also is an ergoline analog similar to LSD, and shows the highest affinity for the 5-HT_{2A} receptor.

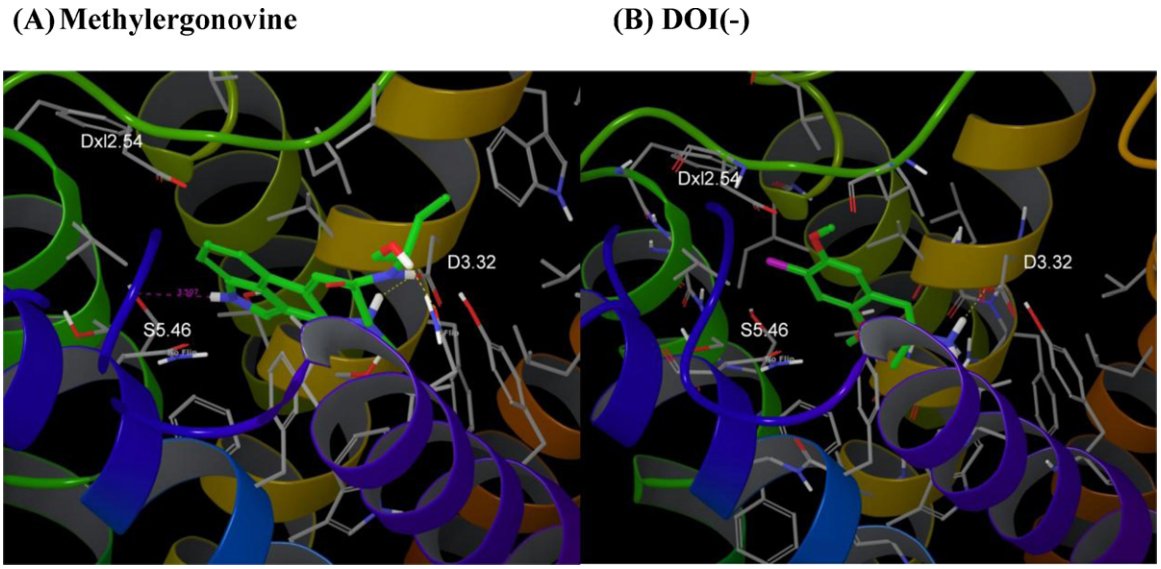

Fig. 7. Docking of selective 5-HT_{2A} inhibitors to the binding site of the 5-HT_{2A} homology model. The ligand is represented in stick form and the carbon atom is green. The residues near the ligand binding pocket are shown as thin sticks, and the subtype-specific residues are labeled.

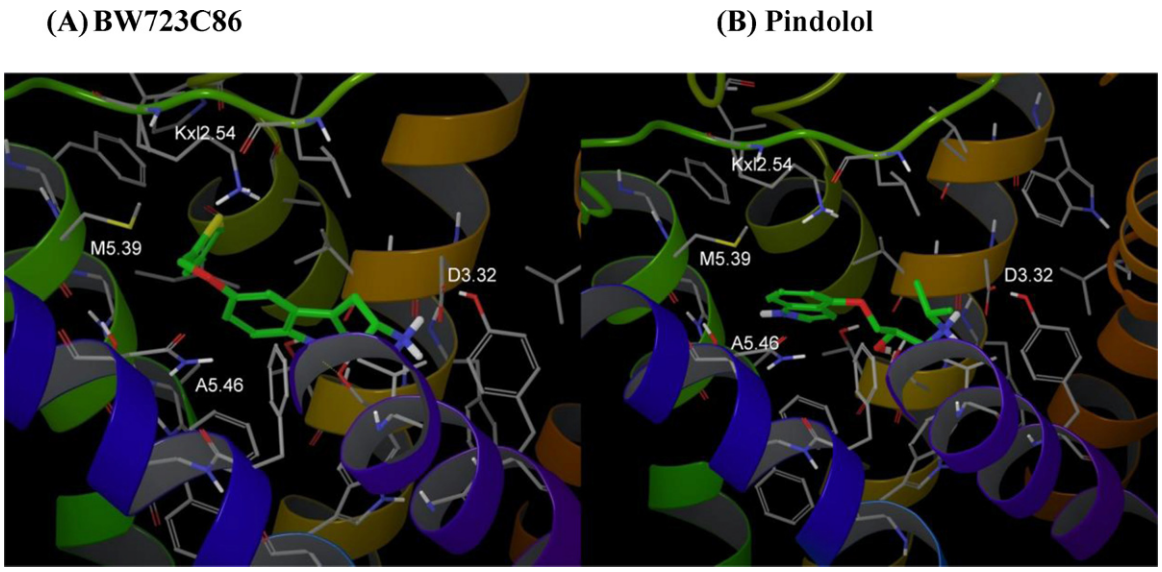

Fig. 8. The docking of selective 5-HT_{2B} inhibitors to the binding site of the 5-HT_{2B} homology model. The ligand is represented in stick format and the carbon atom is green. The residues near the ligand binding pocket are shown as thin sticks and the subtype-specific residues are labeled.

As shown in Fig. 7(A), the subtype-specific residue S5.46 interacts with the NH moiety of methylergonovine, implying the importance of these moieties for selectivity. In the case of 5-HT_{2B} and 5-HT_{2C}, these ligands were less well stabilized due to replacement of serine with alanine, which has no electrostatic interaction with ligands. The NH moiety of LSD was also engaged in hydrogen bonding interaction with the residue. Thus, the 5.46 position of 5-HT_{2A} seems to be important for some selective 5-HT_{2A} agonists.

For compounds containing phenylisopropylamines, such as DOI and DOB, higher affinities to 5-HT_{2A} than to 5-HT_{2B} are explained by the size of the residue at the xl2.54 position. Dxl2.54 at 5-HT_{2A} has less steric hindrance than Kxl2.54 at 5-HT_{2B} because the lysine is more lengthy and bulky, which hinders favorable interaction. The selectivity of this series of compounds to 5-HT_{2C} is not explained by our homology model and docking simulation. Nxl2.54 at 5-HT_{2C} also bears a functional group that can act as a hydrogen bond donor, substantiating its better docking score and experimental affinity for 5-HT_{2C} than for 5-HT_{2B}.

3.5. *Docking of 5-HT_{2B} agonists*

Four selective 5-HT_{2B} agonists were employed in our docking simulation. Among the 5-HT_{2B} agonists, only BW723C86 has been reported as a selective 5-HT_{2B} agonist [60–63]. In addition, we also selected CGS-12066A, pindolol, and quinpirole, because they also exhibit some degree of selectivity over other subtypes, although they possessed low affinity in the references.

The selectivity of 5-HT_{2B} agonists is thought to be attributable to M5.39 and Kxl2.54. Fig. 8 shows the binding mode of BW723C86 and pindolol at the 5-HT_{2B} receptor. In the case of BW723C86, ether moiety is located near the protonated nitrogen of lysine, and methionine has close contact with M5.39. Lysine, the more flexible and longer subtype-specific residue of 5-HT_{2B}, extends to the binding pocket, and is thus located more closely to its electrostatic interaction partner; Dxl2.54 of 5-HT_{2A} and Nxl2.54 of 5-HT_{2C} are a little farther from the binding pocket, thus preferring hydrogen bonding with the ligand partner close to the extracellular side, as shown in the binding mode of DOI. Pindolol interacts with M5.39

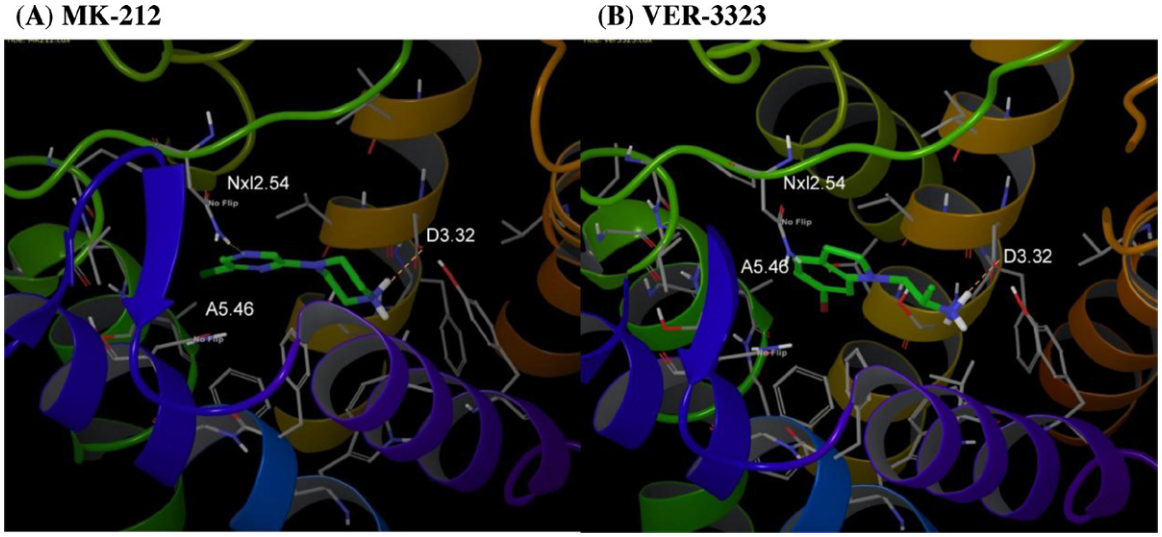

Fig. 9. Docking of selective 5-HT_{2C} inhibitors to the binding site of the 5-HT_{2C} homology model. The ligand is represented in stick format and the carbon atom is green. The residues near the ligand binding pocket are shown as thin sticks and the subtype-specific residues are labeled.

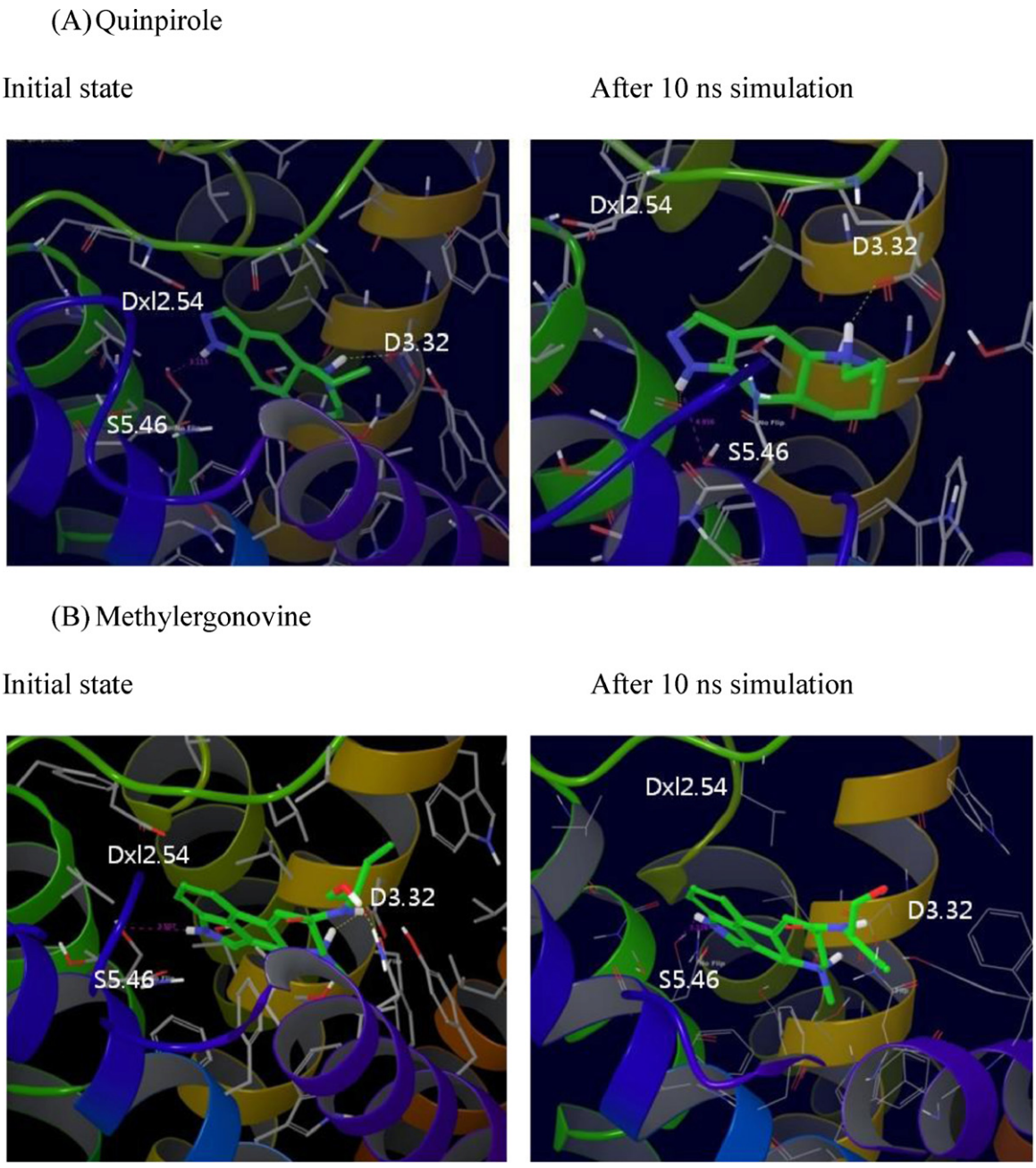

Fig. 10. Binding mode of quinpirole (A) and methylergonovine (B) at the initial state and after 10 ns MD simulation.

and Kxl2.54 by the indole moiety and ether linkage, respectively, which are similar to BW723C86, but the distance appears to be greater.

Reflecting the low affinity of 5-HT_{2B} agonists with the exception of BW723C86, quinpirole had an unexpected docking score, and CGS-12066A failed to find a suitable binding conformation. Quinpirole was the only compound that showed no agreement between its docking scores and experimental biological affinities. Because of hydrogen bonding interaction between the NH atom of the core moiety and S5.46, which we observed in the docking of selective 5-HT_{2A} agonists, it resulted in the highest score in the 5-HT_{2A} receptor. To determine whether S5.46 is a subtype-selective residue that interacts only with 5-HT_{2A} agonists or if it could form a hydrogen bond with any nitrogen atom, we carried out molecular dynamics simulation. The result is described in the molecular dynamics simulation section.

3.6. Docking of 5-HT_{2C} agonists

We selected 5 compounds for our docking simulation of 5-HT_{2C} agonist selectivity. The biological functions of mCPP and MK212, which have an arylpiperazine moiety, have been thoroughly investigated and reported as selective 5-HT_{2C} agonists [64,65]. Ro 60-0175 is also known to be a 5-HT_{2C} agonist, and displayed selectivity over 5-HT_{2B} [66]. Org 37684 is a 5-HT_{2C} agonist, and exhibits moderate selectivity over other 5-HT_2 receptor subtypes [67]. VER-3323 has acted as a 5-HT_{2C} agonist, and produced significant selectivity over the 5-HT_{2A} receptor [68].

Docking studies of the selective 5-HT_{2C} agonists showed that the halogen moieties attached to the opposite side of the protonatable nitrogen point toward the hydrophobic pocket of TM 5, where Ala5.46 lies. This interaction was likely to play an important role in 5-HT_{2C} agonist interaction and selectivity. Fig. 9 illustrates how

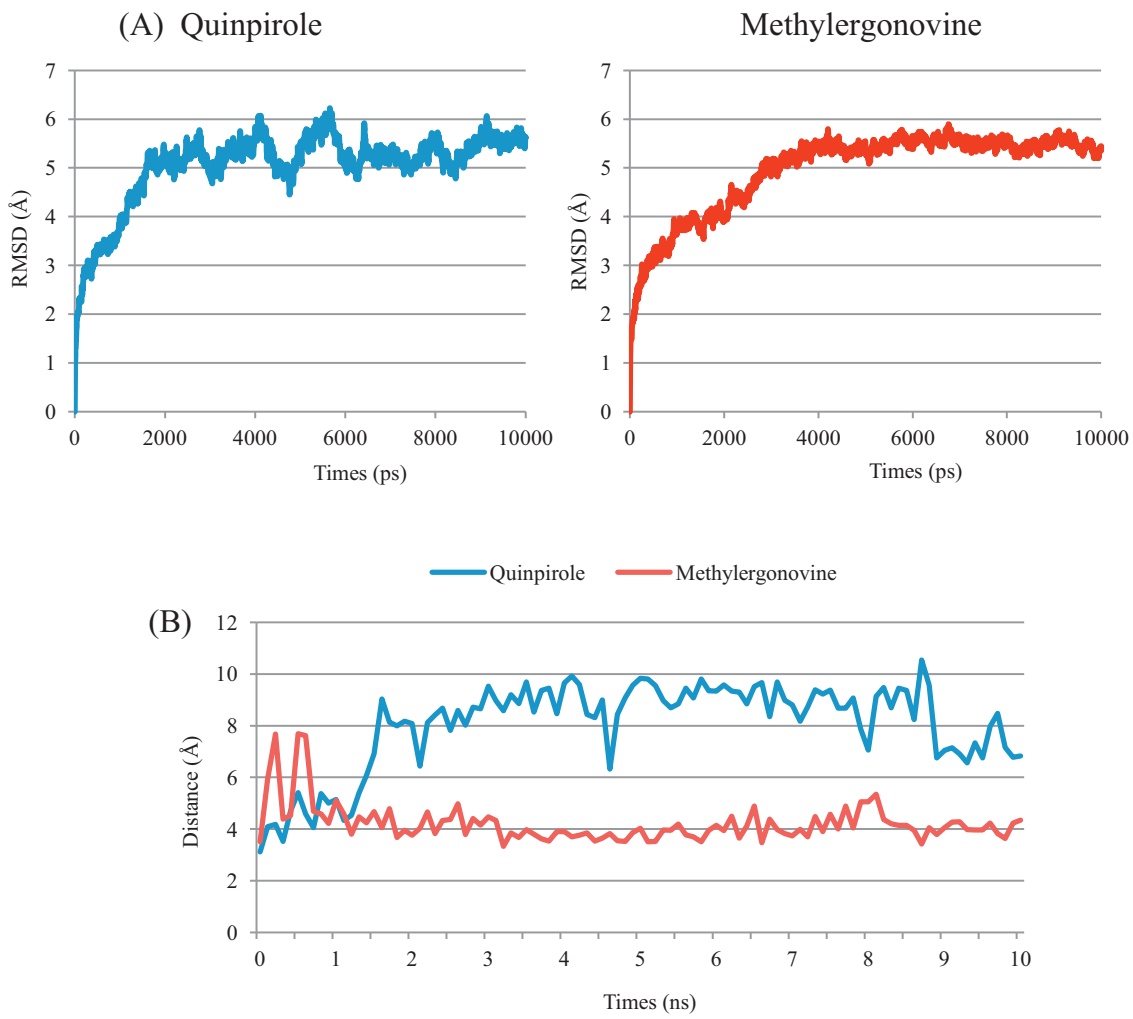

Fig. 11. RMSD of the backbone atoms of the 5-HT_{2A} receptors complexed with the agonists' quinpirole and methylergonovine (A), and a trajectory of the hydrogen bond distance between NH of the ligand (quinpirole and methylergonovine) and Ser5.46 (B).

the chlorine atom of MK-212 is located near the alanine residue and bromine of VER-3323 points toward the same residue. Ala5.46 of the 5-HT_{2C} receptor is replaced by serine in 5-HT_{2A}, thereby reducing the favorable non-polar interaction between ligand and receptor and explaining the selectivity for 5-HT_{2A}. No specific interactions that differentiate the 5-HT_{2C} active site from that of 5-HT_{2B} were observed, as residue position 5.46 of 5-HT_{2B} is also alanine and the residues in EL2 did not contribute to the subtype-selective interaction.

3.7. *Molecular dynamics simulation*

We observed that methylergonovine and LSD interacted with Ser5.46 of 5-HT_{2A} as a selectivity determinant over other subtypes. However, the binding mode of quinpirole also displayed similar interaction and hydrogen bonding between the NH moiety of the ligand and Ser5.46, producing the highest score at this active site (Fig. 10(A)). We need to confirm that hydrogen bond interaction between Ser5.46 and the NH moiety of the ligand is specific to the 5-HT_{2A} agonist. Quinpirole was the only compound for which experimental affinity and docking score did not correlate. Thus, we assumed that the binding mode of quinpirole at 5-HT_{2A} was predicted incorrectly. To find an alternative binding mode, we performed an MD simulation of quinpirole bound to 5-HT_{2A}. For comparison, we also conducted the simulation with methylergonovine and noted significant interaction changes.

MD simulations (10 ns) of both compounds showed that the binding mode of methylergonovine was maintained, whereas that of the quinpirole changed. This observation was consistent with our assumption that the binding mode of quinpirole determined by the docking studies was incorrect. As shown in Fig. 10(A), after 10 ns simulation, quinpirole has moved toward the extracellular side. On the other hand, methylergonovine exhibits similar binding modes between initial (docking conformation) and 10 ns simulation (Fig. 10(B)).

Furthermore, the investigation of protein–ligand interactions during MD simulation suggested that Ser5.46 interacted only with methylergonovine, stressing the importance of this interaction in 5-HT_{2A} agonists. In Fig. 11(A), the RMSD plot of backbone atoms indicates that the complexes achieve equilibrium after 2 ns and 3 ns simulation for quinpirole and methylergonovine, suggesting that analysis of MD results after 3 ns would be more reliable. In Fig. 11(B), the initial distance of both compounds is similar. However, they differ significantly from 1 ns. The distance plot of quinpirole rises suddenly and fluctuates at approximately 8 Å. The binding mode shows that the NH moiety of quinpirole interacts with a different residue, i.e., the backbone of Gly5.42. However, the methylergonovine binding mode is maintained, fluctuating slightly at approximately 4 Å. The binding mode shows that hydrogen

bonding interaction between the NH moiety of the ligand and Ser5.46 was maintained. This distance graph tells us that hydrogen bonding interaction of methylergonovine is maintained, while that of quinpirole is broken. The glide score of this changed binding mode of quinpirole was −5.96, which was a 1.02 deterioration of glide score from the initial state. We speculate this is due to fewer van der Waals interactions with nearby residues, caused by the more exposed binding mode toward the extracellular side. This score was less than the glide score of quinpirole at 5-HT_{2B} and is consistent with the fact that quinpirole is a selective 5-HT_{2B} agonist.

4. Conclusion

A computational study was performed to elucidate the structural basis of 5-HT_2 agonist selectivity. A comparative homology modeling technique was adopted to build the 3-dimensional protein structures. Among the available GPCR crystal structures to be used as a template for model construction, the β_2-adrenergic receptor was the most suitable. Using this template we performed a sequence alignment and found that the identities between the transmembrane regions of the targets and template were approximately 40% for every subtype, suggesting that the generated models would be reliable. The amino acid sequence alignment and superimposition of resulting protein structures suggested that 3 regions were likely to influence 5-HT_2 agonist selectivity: xl2.54, 5.39, and 5.46. They differed in charge states, hydrophobicity, and flexibility. Subsequent protein–ligand docking simulations demonstrated that 5-HT_2 agonist selectivity arose from these residues. Ser5.46 and Dxl2.54 of the 5-HT_{2A} receptor showed preferential interaction with 5-HT_{2A} agonists. In the case of the 5-HT_{2B} receptor, the long and flexible Kxl2.54 and M5.39 contributed to polar and hydrophobic interactions with ligands. The halogen moiety of the 5-HT_{2C} agonist specifically interacted with Ala5.46, and the higher hydrophobic docking score of 5-HT_{2C} agonist confirmed the specific non-polar interaction between alanine residues and ligand in the 5-HT_{2C} receptor. MD simulations of quinpirole and methylergonovine verified that Ser5.46 is a specific residue for 5-HT_{2A} agonists. We found that this residue preferentially interacted with methylergonovine, a selective 5-HT_{2A} agonist, rather than quinpirole, a selective 5-HT_{2B} agonist. This validated our observations from the docking studies of 5-HT_{2A} agonist. This knowledge of subtype-selective residues and their influence on ligand binding should be helpful in the development of subtype-selective 5-HT_2 agonists.

Acknowledgement

This project was supported by Korea Institute of Science and Technology.

Appendix A. Supplementary data

Supplementary data associated with this article can be found, in the online version, at http://dx.doi.org/10.1016/j.jmgm.2012.06.006.

References

[1] Drug Information Online, www.drugs.com (accessed 2010).
[2] M.C. Lagerstrom, H.B. Schioth, Structural diversity of G protein-coupled receptors and significance for drug discovery, Nature Reviews Drug Discovery 7 (2008) 339–357.
[3] B. Bakir, O. Sezerman, in: F. Rothlauf, J. Branke, S. Cagnoni, E. Costa, C. Cotta, R. Drechsler, et al. (Eds.), Functional classification of G-protein coupled receptors, based on their specific ligand coupling patterns applications of evolutionary computing, Vol. 3907, Springer, Berlin/Heidelberg, 2006, pp. 1–12.
[4] V. Katritch, I. Kufareva, R. Abagyan, Structure based prediction of subtype-selectivity for adenosine receptor antagonists, Neuropharmacology 60 (2011) 108–115.
[5] M. Berger, J.A. Gray, B.L. Roth, The expanded biology of serotonin, Annual Review of Medicine 60 (2009) 355–366.
[6] D. Hoyer, G. Martin, 5-HT receptor classification and nomenclature: towards a harmonization with the human genome, Neuropharmacology 36 (1997) 419–428.
[7] B.L. Roth, Multiple serotonin receptors: clinical and experimental aspects, Ann.Clin. Psychiatry. 1994 (1994) 12.
[8] N.M. Appel, W.M. Mitchell, R.K. Garlick, R.A. Glennon, M. Teitler, E.B. De Souza, Autoradiographic characterization of (±)-1-(2,5-dimethoxy-4-[125I] iodophenyl)-2-aminopropane ([125I]DOI) binding to 5-HT_2 and 5-HT_{1c} receptors in rat brain, Journal of Pharmacology and Experimental Therapeutics 255 (1990) 843–857.
[9] D.E. Nichols, Hallucinogens, Pharmacology and Therapeutics 101 (2004) 131–181.
[10] B.M. Smith, J.M. Smith, J.H. Tsai, J.A. Schultz, C.A. Gilson, S.A. Estrada, et al., Discovery and structure–activity relationship of (1R)-8-chloro-2,3,4,5-tetrahydro-1-methyl-1H-3-benzazepine (Lorcaserin), a selective serotonin 5-HT_{2C} receptor agonist for the treatment of obesity, Journal of Medicinal Chemistry 51 (2007) 305–313.
[11] R.B. Rothman, M.H. Baumann, J.E. Savage, L. Rauser, A. McBride, S.J. Hufeisen, et al., Evidence for possible involvement of 5-HT_{2B} receptors in the cardiac valvulopathy associated with fenfluramine and other serotonergic medications, Circulation 102 (2000) 2836–2841.
[12] B.L. Roth, Drugs and valvular heart disease, New England Journal of Medicine 356 (2007) 6–9.
[13] N. Weissman, Appetite suppressant valvulopathy: a review of current data, Cardiovascular Reviews and Reports 20 (1999) 146–155.
[14] B.A. Rocha, E.H. Goulding, L.E. O'Dell, A.N. Mead, N.G. Coufal, L.H. Parsons, et al., Enhanced locomotor, reinforcing, and neurochemical effects of cocaine in serotonin 5-hydroxytryptamine 2C receptor mutant mice, Journal of Neuroscience 22 (2002) 10039–10045.
[15] L.H. Tecott, L.M. Sun, S.F. Akana, A.M. Strack, D.H. Lowenstein, M.F. Dallman, et al., Eating disorder and epilepsy in mice lacking 5-HT_{2C} serotonin receptors, Nature 374 (1995) 542–546.
[16] J.M. Chou-Green, T.D. Holscher, M.F. Dallman, S.F. Akana, Compulsive behavior in the 5-HT_{2C} receptor knockout mouse, Physiology and Behavior 78 (2003) 641–649.
[17] P.L. Delgado, M.F. Hallucinogens, serotonin and obsessive–compulsive disorder, Journal of Psychoactive Drugs 30 (1998) 359–366.
[18] J.R. Martin, M. Bös, F. Jenck, J.-L. Moreau, V. Mutel, A.J. Sleight, et al., 5-HT_{2C} receptor agonists: pharmacological characteristics and therapeutic potential, Journal of Pharmacology and Experimental Therapeutics 286 (1998) 913–924.
[19] D.A. Shapiro, B.L. Roth, Insights into the structure and function of 5-HT_2 family-serotonin receptors reveal novel strategies for therapeutic target development, Expert Opinion on Therapeutic Targets 5 (2001) 685–695.
[20] K.J. Miller, Serotonin 5-HT_{2C} receptor agonists: potential for the treatment of obesity, Molecular Interventions 5 (2005) 282–291.
[21] B.L. Roth, E. Lopez, S. Patel, W.K. Kroeze, The multiplicity of serotonin receptors: uselessly diverse molecules or an embarrassment of riches, The Neuroscientist 6 (2000) 252–262.
[22] M. Isaac, Serotonergic 5-HT_{2C} receptors as a potential therapeutic target for the design antiepileptic drugs, Current Topics in Medicinal Chemistry 5 (2005) 59–67.
[23] M.J. Millan, J.-L. Peglion, G. Lavielle, S. Perrin-Monneyron, 5-HT_{2C} receptors mediate penile erections in rats: actions of novel and selective agonists and antagonists, European Journal of Pharmacology 325 (1997) 9–12.
[24] M. Rashid, P. Manivet, H. Nishio, J. Pratuangdejkul, M. Rajab, M. Ishiguro, et al., Identification of the binding sites and selectivity of sarpogrelate, a novel 5-HT_2 antagonist, to human 5-HT_{2A}, 5-HT_{2B} and 5-HT_{2C} receptor subtypes by molecular modeling, Life Sciences 73 (2003) 193–207.
[25] B. Kobilka, G.F.X. Schertler, New G-protein-coupled receptor crystal structures: insights and limitations, Trends in Pharmacological Sciences 29 (2008) 79–83.
[26] J.C. Mobarec, R. Sanchez, M. Filizola, Modern homology modeling of G-protein coupled receptors: which structural template to use, Journal of Medicinal Chemistry 52 (2009) 5207–5216.
[27] E.Y.T. Chien, W. Liu, Q. Zhao, V. Katritch, G. Won Han, M.A. Hanson, et al., Structure of the human dopamine D3 receptor in complex with a D2/D3 selective antagonist, Science 330 (2010) 1091–1095.
[28] S.G.F. Rasmussen, H.-J. Choi, D.M. Rosenbaum, T.S. Kobilka, F.S. Thian, P.C. Edwards, et al., Crystal structure of the human β2 adrenergic G-protein-coupled receptor, Nature 450 (2007) 383–387.
[29] V. Cherezov, D.M. Rosenbaum, M.A. Hanson, S.G.F. Rasmussen, F.S. Thian, T.S. Kobilka, et al., High-resolution crystal structure of an engineered human β2-adrenergic G protein-coupled receptor, Science 318 (2007) 1258–1265.
[30] D.M. Rosenbaum, V. Cherezov, M.A. Hanson, S.G.F. Rasmussen, F.S. Thian, T.S. Kobilka, et al., GPCR engineering yields high-resolution structural insights into β2-adrenergic receptor function, Science 318 (2007) 1266–1273.
[31] T. Warne, M.J. Serrano-Vega, J.G. Baker, R. Moukhametzianov, P.C. Edwards, R. Henderson, et al., Structure of a β1-adrenergic G-protein-coupled receptor, Nature 454 (2008) 486–491.

[32] V.-P. Jaakola, M.T. Griffith, M.A. Hanson, V. Cherezov, E.Y.T. Chien, J.R. Lane, et al., The 2.6 Angstrom crystal structure of a human A2A adenosine receptor bound to an antagonist, Science 322 (2008) 1211–1217.
[33] K. Palczewski, T. Kumasaka, T. Hori, C.A. Behnke, H. Motoshima, B.A. Fox, et al., Crystal structure of rhodopsin: a G protein-coupled receptor, Science 289 (2000) 739–745.
[34] B. Wu, E.Y.T. Chien, C.D. Mol, G. Fenalti, W. Liu, V. Katritch, et al., Structures of the CXCR4 chemokine GPCR with small-molecule and cyclic peptide antagonists, Science 330 (2010) 1066–1071.
[35] T. Shimamura, M. Shiroishi, S. Weyand, H. Tsujimoto, G. Winter, V. Katritch, et al., Structure of the human histamine H1 receptor complex with doxepin, Nature 475 (2011) 65–70.
[36] K. Haga, A.C. Kruse, H. Asada, T. Yurugi-Kobayashi, M. Shiroishi, C. Zhang, et al., Structure of the human M2 muscarinic acetylcholine receptor bound to an antagonist, Nature 482 (2012) 547–551.
[37] A. Manglik, A.C. Kruse, T.S. Kobilka, F.S. Thian, J.M. Mathiesen, R.K. Sunahara, et al., Crystal structure of the μ-opioid receptor bound to a morphinan antagonist, Nature 485 (2012) 321–326.
[38] H. Wu, D. Wacker, M. Mileni, V. Katritch, G.W. Han, E. Vardy, et al., Structure of the human κ-opioid receptor in complex with JDTic, Nature 485 (2012) 327–332.
[39] K. Reynolds, V. Katritch, R. Abagyan, Identifying conformational changes of the β_2 adrenoceptor that enable accurate prediction of ligand/receptor interactions and screening for GPCR modulators, Journal of Computer-Aided Molecular Design 23 (2009) 273–288.
[40] D.G. Higgins, J.D. Thompson, T.J. Gibson, Using CLUSTAL for multiple sequence alignments, in: F.D. Russell (Ed.), Methods in Enzymology, vol. 266, Academic Press, 1996, pp. 383–402.
[41] J.M. Baldwin, G.F.X. Schertler, V.M. Unger, An alpha-carbon template for the transmembrane helices in the rhodopsin family of G-protein-coupled receptors, Journal of Molecular Biology 272 (1997) 144–164.
[42] A. Sali, T.L. Blundell, Comparative protein modelling by satisfaction of spatial restraints, Journal of Molecular Biology 234 (1993) 779–815.
[43] J.A. Ballesteros, H. Weinstein, Integrated methods for the construction of three-dimensional models and computational probing of structure-function relations in G protein-coupled receptors, in: C.S. Stuart (Ed.), Methods in Neurosciences, vol. 25, Academic Press, 1995, pp. 366–428.
[44] J.W. Ponder, F.M. Richards, Tertiary templates for proteins: use of packing criteria in the enumeration of allowed sequences for different structural classes, Journal of Molecular Biology 193 (1987) 775–791.
[45] Jorgensen, W.L. Maxwell, D.S. Tirado-Rives, J. Development, Testing of the OPLS all-atom force field on conformational energetics and properties of organic liquids, Journal of the American Chemical Society 118 (1996) 11225–11236.
[46] R.A. Laskowski, M.W. MacArthur, D.S. Moss, J.M. Thornton, PROCHECK: a program to check the stereochemical quality of protein structures, Journal of Applied Crystallography 26 (1993) 283–291.
[47] L.M. Gregoret, F.E. Cohen, Novel method for the rapid evaluation of packing in protein structures, Journal of Molecular Biology 211 (1990) 959–974.
[48] Maestro v9. 0, Schrodinger Inc., Portland, OR, 2010.
[49] ConfGen 2. 2, Schrodinger Inc, Portland, OR, 2010.
[50] R.A. Friesner, R.B. Murphy, M.P. Repasky, L.L. Frye, J.R. Greenwood, T.A. Halgren, et al., Extra precision glide: docking and scoring incorporating a model of hydrophobic enclosure for protein–ligand complexes, Journal of Medicinal Chemistry 49 (2006) 6177–6196.
[51] D. Shortle, K.T. Simons, D. Baker, Clustering of low-energy conformations near the native structures of small proteins, Proceedings of the National Academy of Sciences of the United States of America 95 (1998) 11158–11162.
[52] N. Almaula, B.J. Ebersole, J.A. Ballesteros, H. Weinstein, S.C. Sealfon, Contribution of a helix 5 locus to selectivity of hallucinogenic and nonhallucinogenic ligands for the human 5-hydroxytryptamine2A and 5-hydroxytryptamine2C receptors: direct and indirect effects on ligand affinity mediated by the same locus, Molecular Pharmacology 50 (1996) 34–42.
[53] D.A. Shapiro, K. Kristiansen, W.K. Kroeze, B.L. Roth, Differential modes of agonist binding to 5-hydroxytryptamine2A serotonin receptors revealed by mutation and molecular modeling of conserved residues in transmembrane region 5, Molecular Pharmacology 58 (2000) 877–886.
[54] P. Manivet, B.t. Schneider, J.C. Smith, D.-S. Choi, L. Maroteaux, O. Kellermann, et al., The serotonin binding site of human and murine 5-HT_{2B} receptors, Journal of Biological Chemistry 277 (2002) 17170–17178.
[55] A.R. Knight, A. Misra, K. Quirk, K. Benwell, D. Revell, G. Kennett, et al., Pharmacological characterisation of the agonist radioligand binding site of 5-HT_{2A}, 5-HT_{2B} and 5-HT_{2C} receptors, Naunyn–Schmiedeberg's Archives of Pharmacology 370 (2004) 114–123.
[56] C.T. Egan, K. Herrick-Davis, K. Miller, R.A. Glennon, M. Teitler, Agonist activity of LSD and lisuride at cloned $5HT_{2A}$ and $5HT_{2C}$ receptors, Psychopharmacology 136 (1998) 409–414.
[57] M. Titeler, R.A. Lyon, R.A. Glennon, Radioligand binding evidence implicates the brain 5-HT_2 receptor as a site of action for LSD and phenylisopropylamine hallucinogens, Psychopharmacology 94 (1988) 213–216.
[58] B. Sadzot, J.M. Baraban, R.A. Glennon, R.A. Lyon, S. Leonhardt, C.-R. Jan, et al., Hallucinogenic drug interactions at human brain 5-HT_2 receptors: implications for treating LSD-induced hallucinogenesis, Psychopharmacology 98 (1989) 495–499.
[59] G.J. Marek, G.K. Aghajanian, LSD and the phenethylamine hallucinogen DOI are potent partial agonists at 5-HT_{2A} receptors on interneurons in rat piriform cortex, Journal of Pharmacology and Experimental Therapeutics 278 (1996) 1373–1382.
[60] G.A. Kennett, M.D. Wood, F. Bright, B. Trail, G. Riley, V. Holland, et al., SB 242084, a selective and brain penetrant 5-HT_{2C} receptor antagonist, Neuropharmacology 36 (1997) 609–620.
[61] G.A. Kennett, K. Ainsworth, B. Trail, T.P. Blackburn, BW 723C86, a 5-HT_{2B} receptor agonist, causes hyperphagia and reduced grooming in rats, Neuropharmacology 36 (1997) 233–239.
[62] R.H.P. Porter, K.R. Benwell, H. Lamb, C.S. Malcolm, N.H. Allen, D.F. Revell, et al., Functional characterization of agonists at recombinant human 5-HT_{2A}, 5-HT_{2B} and 5-HT_{2C} receptors in CHO-K1 cells, British Journal of Pharmacology 128 (1999) 13–20.
[63] J.C. Jerman, S.J. Brough, T. Gager, M. Wood, M.C. Coldwell, D. Smart, et al., Pharmacological characterisation of human 5-HT_2 receptor subtypes, European Journal of Pharmacology 414 (2001) 23–30.
[64] G. Kennett, G. Curzon, Evidence that hypophagia induced by mCPP and TFMPP requires 5-HT_{1C} and 5-HT_{1B} receptors; hypophagia induced by RU 24969 only requires 5-HT_{1B} receptors, Psychopharmacology 96 (1988) 93–100.
[65] I. Lucki, H.R. Ward, A. Frazer, Effect of 1-(m-chlorophenyl)piperazine and 1-(m-trifluoromethylphenyl)piperazine on locomotor activity, Journal of Pharmacology and Experimental Therapeutics 249 (1989) 155–164.
[66] M. Bös, F. Jenck, J.R. Martin, J.-L. Moreau, A.J. Sleight, J. Wichmann, et al., Novel agonists of $5HT_{2C}$ receptors. Synthesis and biological evaluation of substituted 2-(indol-1-yl)-1-methylethylamines and 2-(indeno[1,2-b]pyrrol-1-yl)-1-methylethylamines. Improved therapeutics for obsessive compulsive disorder, Journal of Medicinal Chemistry 40 (1997) 2762–2769.
[67] J. De Vry, R. Schreiber, Effects of selected serotonin 5-HT_1 and 5-HT_2 receptor agonists on feeding behavior: possible mechanisms of action, Neuroscience and Biobehavioral Reviews 24 (2000) 341–353.
[68] J.M. Bentley, D.R. Adams, D. Bebbington, K.R. Benwell, M.J. Bickerdike, J.E.P. Davidson, et al., Indoline derivatives as 5-HT_{2C} receptor agonists, Bioorganic and Medicinal Chemistry Letters 14 (2004) 2367–2370.